Available online at www.sciencedirect.com

SCIENCE DIRECT®

Journal of Catalysis 228 (2004) 152–161

JOURNAL OF CATALYSIS

www.elsevier.com/locate/jcat

Nature of catalyst deactivation during citral hydrogenation: a catalytic and ATR-IR study

Marco Burgener, Ronny Wirz, Tamas Mallat, Alfons Baiker *

Department of Chemistry and Applied Biosciences, Swiss Federal Institute of Technology, ETH Hönggerberg, CH-8093 Zurich, Switzerland

Received 22 June 2004; revised 1 September 2004; accepted 2 September 2004

Abstract

Deactivation of a 5 wt% Pd/Al_2O_3 catalyst during hydrogenation of citral (**1**) to citronellal (**2**), 3,7-dimethyl-2-octenal (**3**), and dihydrocitronellal (**4**) has been studied in a continuous-flow fixed-bed reactor. The reactions were carried out at 40 °C and 190 bar in hexane, "supercritical" CO_2, or ethane as solvents. ATR-IR spectroscopic analysis of the solid/liquid interphase under reaction conditions at low pressure revealed that **1** and **3** decarbonylate on the Pd surface resulting in strongly adsorbed CO and C_xH_y-type hydrocarbon fragments. The absence of decarbonylation products from **2** and **4** and the excellent chemoselectivity for the hydrogenation of the C=C bonds are interpreted by adsorption of the molecules in a tilted position on Pd, π-bonded via one C=C bond (**2**) or di-π-bonded via the C=C–C=O fragment (**1** and **3**). A practically important observation is that a short reoxidation by air of the used Pd/Al_2O_3 under very mild conditions (40 °C, 6 bar) can circumvent further deactivation, but the original activity cannot be regained. All these observations indicate that the irreversible deactivation of Pd/Al_2O_3 cannot be traced to CO poisoning. We propose that site blocking caused by heavier oligomeric surface products is the major reason for the observed catalyst deactivation.

Keywords: Hydrogenation; Catalyst deactivation; ATR-IR spectroscopy; Pd/Al_2O_3; Citral; Supercritical carbon dioxide; Supercritical ethane

1. Introduction

Selective hydrogenation of α,β-unsaturated aldehydes is an important process in the preparation of intermediates and fine chemicals [1–3]. Since hydrogenation of the C=C bond is thermodynamically favored to that of the C=O bond over the usual metal hydrogenation catalysts, appropriate design of catalyst composition and the control of reaction conditions are important to obtain the desired product.

Citral (**1**, Scheme 1) is a fascinating example of an α,β-unsaturated aldehyde, since it has three different double bonds: an isolated and a conjugated C=C double bond, and a carbonyl group. Citral and its hydrogenated intermediates are important in the perfumery industry [4,5]. Beside the parallel and consecutive hydrogenation of the C=C and C=O bonds, the aliphatic aldehydes citronellal (**2**) and dihydrocitronellal (**4**) can react with an alcoholic solvent to form an acetal (not shown), or cyclization of citronellal produces isopulegol. These acid-catalyzed side reactions can be controlled by the proper choice of the metal precursor and the support, and the hydrophobic character of the solvent [6–8].

Selective hydrogenation of citral has been the topic of numerous studies in the past years. Several reports have appeared on the selectivity of mono- [7,9–13] and bimetallic [14–18] catalysts, the role of catalyst supports [5,19,20] and various promoters [19,21–23], the effect of solvents including ionic liquids [24] and supercritical CO_2 [25,26], and the kinetic [12,27–29] and mechanistic [30] aspects of this transformation. It has been shown that Pd is the most active metal for citral hydrogenation [10] and highly selective to C=C bond hydrogenation, affording citronellal and dihydrocitronellal in good yields [23,31].

---

[*] Corresponding author. Fax: +41 1 632 11 63.
E-mail address: baiker@chem.ethz.ch (A. Baiker).

0021-9517/$ – see front matter © 2004 Elsevier Inc. All rights reserved.
doi:10.1016/j.jcat.2004.09.006

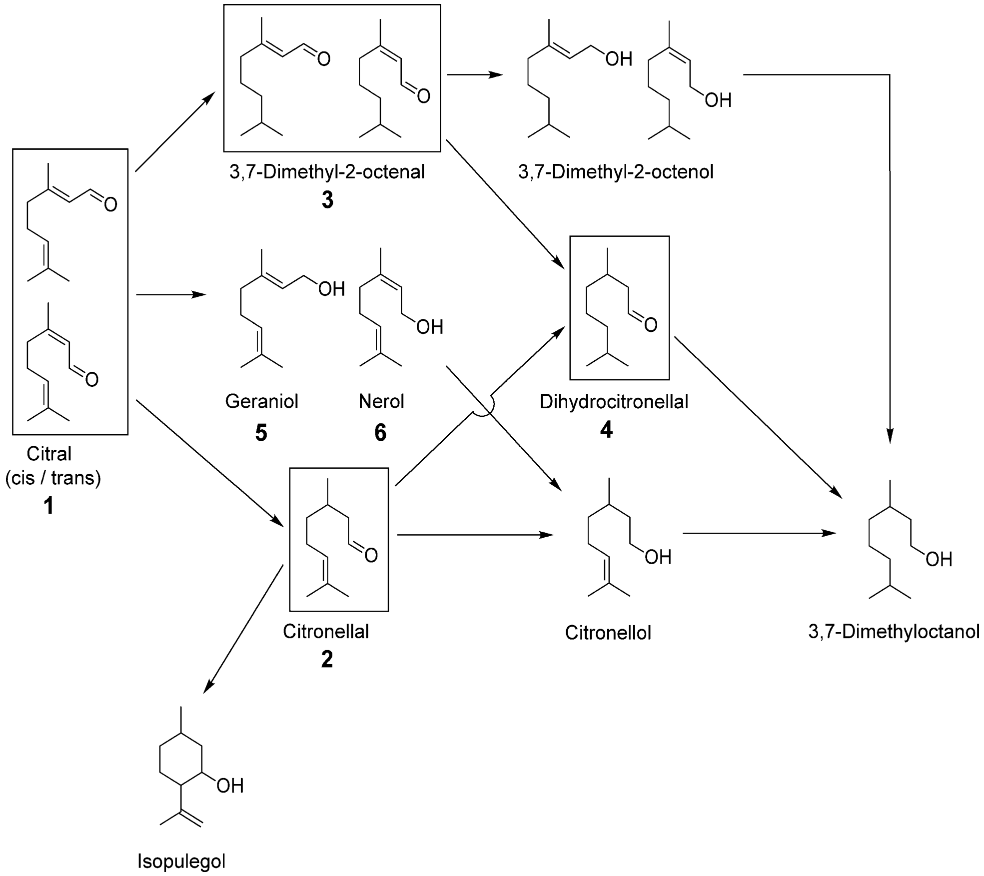

Scheme 1. Reaction network of citral hydrogenation over Pt-group metal catalysts. Only the compounds in rectangles could be detected when using Pd/Al_2O_3 [41].

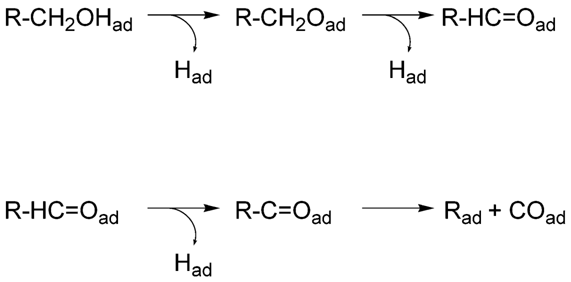

Scheme 2. Simplified route of the decomposition (decarbonylation) of a primary alcohol via the aldehyde on the Pt-group metal surface.

Catalyst deactivation has been barely investigated though the phenomenon seems to be typical for most metal hydrogenation catalysts [10,32,33]. Singh and Vannice assumed [10,32] that decomposition of either the citral or the unsaturated alcohols geraniol (**5**) and nerol (**6**) was responsible for the loss of catalytic activity of silica-supported group VIII metals. The proposal was based on extensive surface science studies of the decomposition (decarbonylation) of alcohols and aldehydes on various Pt-group metal surfaces [34–39]. According to Davis and Barteau [40], decomposition of alcohols and aldehydes via an adsorbed acyl species results in CO and C_xH_y-type hydrocarbon fragments (Scheme 2).

The present study is a continuation of our former investigation of citral hydrogenation in a continuous-flow fixed-bed reactor using “supercritical” and conventional solvents [41]. Catalyst deactivation with time on stream was found to be a general feature of various Pt-group metal catalysts, including the most active Pd/Al_2O_3. The aim of the present work is to get more information on the nature of catalyst deactivation. The continuous-flow reactor is ideally suited for studying the gradual loss of activity. Beside the catalytic investigations we applied ATR-IR spectroscopy under close to in situ conditions (at 1 bar) to understand the processes at the molecular level. In contrast to standard IR spectroscopy where the infrared beam passes directly through the sample, in the attenuated total reflection (ATR) mode the infrared radiation is passed through an internal reflection element, an infrared transparent crystal of high refractive index, which is in contact with the sample [42]. The very short pathlength used in ATR-IR spectroscopy makes this technique surface sensitive and hence suitable for characterization of heterogeneous catalysts [43,44]. ATR-IR is ideally suited for vibrational spectroscopy at the solid-liquid interface since the evanescent wave selectively probes the region near the interface, keeping in this way the contribution from the liquid phase reasonably small.

2. Experimental

2.1. Materials

Citral (96%, Aldrich, $cis/trans = 0.6$), citronellal (93%, Acros), nerol (97%, ABCR), geraniol (99%, Acros), n-hexane (96%, Scharlau), ethyl acetate (99.5%, Merck), 5 wt% Pd/Al_2O_3 (Fluka, mean particle diameter of ca. 32 µm, metal dispersion: 0.35, as determined by transmission electron microscopy), Al_2O_3 (Merck, anhydrous γ-alumina, particle diameter of ca. 90 µm), carbon dioxide (99.9%, PanGas), ethane (99.5%, Linde), hydrogen (99.99%, PanGas) and synthetic air (80% N_2, 20% O_2) were used as delivered.

Dihydrocitronellal (94% by GC analysis) was synthesized by hydrogenation of citral in a batch reactor under the following conditions: 1 mL citral, 5 mL diethyl ether, 42 mg 5 wt% Pd/Al_2O_3, 40 bar, room temperature, 2 h.

2.2. Catalytic studies in the continuous high-pressure reactor system

Hydrogenation of citral and citronellal was carried out in a computer-controlled continuous-flow reactor system. Basically, the system consisted of a vertically mounted reactor section (down-stream concept) and an automatic sampling system at the outlet of the reactor. The experimental setup has been described elsewhere [45].

All feed streams were combined in a mixing chamber before entering in the reactor section. The tubular reactor (stainless steel) was closed by steel frits toward both ends and the inner diameter was 10 mm. The catalyst (0.1 g 5 wt% Pd/Al_2O_3 diluted with 2.5 g Al_2O_3) was fixed by quartz wool plugs, resulting in a catalyst bed length L of ca. 15 mm and an $L/\mathrm{dp} = 470$ (dp: particle diameter). The space time-related quantity W/F was typically 1.2 $\mathrm{g\,h\,mol^{-1}}$ (W, catalyst mass; F, molar feed rate). Temperature was controlled separately for the mixing chamber and the reactor section using two independent thermostats (Julabo type HD-4 and type F32-HD, respectively). The pressure was kept constant by a backpressure regulator (Tescom series 26-1700). Citral and citronellal were pumped into the reactor system by an HPLC pump (Jasco PU-980).

Standard reaction conditions were as follows: $T = 40\,^\circ\mathrm{C}$, $p = 190$ bar, solvent (CO_2 or ethane) flow $= 157$ $\mathrm{nL\,h^{-1}}$, reactant (citral or citronellal) flow $= 10.7$ and 10.9 $\mathrm{g\,h^{-1}}$, respectively, H_2 flow $= 7.8$ $\mathrm{nL\,h^{-1}}$, corresponding to a molar ratio reactant: H_2:solvent of 1:5:100. For the measurement in hexane, the supercritical fluid was replaced by nitrogen and the solvent mass flow was set to 38 $\mathrm{g\,h^{-1}}$, corresponding to a volume ratio of citral: solvent = 1:3.

Sampling occurred automatically every hour. After dilution with ethyl acetate the samples were analyzed by a GC (HP 6890) equipped with a capillary column (HP-FFAP; 0.25 µm, 30 m, 0.32 mm), an autosampling device (HP 7683), a split/splitless injector, and a flame ionization detector. The selectivity was defined as Y_i/X_i (Y_i yield of a product, X_i conversion of citral (citronellal)). For each experiment fresh catalyst was used.

For the catalyst reactivation experiment the reactor was filled with fresh catalyst and the reaction was started under standard conditions. After 3 h the citral flow and the gas feed were stopped, and the catalyst bed was flushed with a synthetic air flow for 10 min at 6 bar. After the oxidation step, the conditions for the hydrogenation of citral were reset again.

2.3. Phase behavior study

In our former article we studied the phase behavior of the reaction mixtures in citral hydrogenation [41]. The measurements were carried out in a high-pressure view cell of variable volume (22–62 mL). The whole diameter was covered with a sapphire window which allowed observation of even liquid droplets. The system was computer-controlled and equipped with online digital video imaging and recording. The details of the view cell have been described before [46].

Note that the commonly used term supercritical is defined only for pure component systems [47]. In multicomponent systems this term is deprived of any meaning, since phase separation is still possible under conditions beyond the mixture critical point or the critical points of the pure components. Here we use this expression, in quotes, for a single phase at temperatures above the mixture critical point.

2.4. ATR-IR spectroscopy

Before film preparation the Pd/Al_2O_3 catalyst was crushed and subsequently preactivated in flowing H_2 for 1 h (after purging with Ar for 30 min) at 400 °C. The film was prepared by dropping a slurry of catalyst in THF (Fluka, puriss) on the ATR crystal, a $50 \times 20 \times 2$ mm ZnSe plate (45°, Komlas), and then THF was evaporated under vacuum. Assuming refractive indices of 1.4 for the wet film and 2.4 for ZnSe, a penetration depth d_p of 1.7 µm (0.6 µm) at 1000 $\mathrm{cm^{-1}}$ (3000 $\mathrm{cm^{-1}}$) was calculated.

Infrared spectra were measured on a Bruker IFS 66/S FTIR spectrometer equipped with a dedicated ATR-IR attachment (Optispec) and an MCT detector cooled by liquid nitrogen. All spectra were recorded by coaddition of 200 scans at a resolution of 4 $\mathrm{cm^{-1}}$. The ZnSe prism was fixed in a homemade stainless steel flow cell [48]. The gap between the polished steel surface of the cell and the ZnSe prism was 250 µm and defined by a 30×1 mm viton O-ring (Johannsen AG) fit into a precision electro-eroded nut of the steel cell. The total volume of the cell was 0.077 mL. The flowthrough cell was thermostated and all measurements were performed at 30 °C. The liquid flow was controlled by a peristaltic pump (ISMATEC Reglo 100) located behind the cell (1 mL/min). Liquid was provided from two separate glass bubble tanks; one contained the solvent only and the other the dissolved reactant. The flow from the two tanks was determined by two computer-controlled pneumatically actuated three-way Teflon valves (Parker PV-1-2324). Steel tubing was used throughout the setup to avoid oxygen diffusion into the cell.

First nitrogen-saturated hexane was flown over the catalyst till the ATR-IR spectra were stable. Hexane was then saturated with hydrogen and the catalyst surface was reduced for 10 min. During this step some unidentified species were removed from the surface as evidenced by changes in the spectra. The spectrum collected at the end of this procedure served as the reference for the following spectra. Then a hydrogen-saturated solution of the corresponding reactant (0.1 mL in 50 mL hexane) was flown over the catalyst film and the reactions were monitored for about 30 min.

For transmission experiments a normal sample holder replaced the ATR-IR attachment. A variable pathlength IR cell (SPECAC) with KBr windows was used with a pathlength adjusted to about 100 µm. The concentration was 100 µl in 5 mL hexane.

3. Results

3.1. Deactivation of Pd/Al_2O_3 during citral hydrogenation in various solvents

Hydrogenation of citral (Scheme 1) was studied in a continuous-flow fixed-bed reactor using a 5 wt% Pd/Al_2O_3. This catalyst was the most active among various supported Pt-group metals tested [41]. Further advantage of Pd/Al_2O_3 is the high selectivity in the saturation of the C=C bonds of citral. None of the unsaturated or saturated alcohols depicted in Scheme 1 could be detected by GC analysis and the cumulative selectivity to the main products citronellal, 3,7-dimethyl-2-octenal, and dihydrocitronellal reached 95–100% in the supercritical fluids (CO_2: $T_c = 30.9\,°C$, $p_c = 73.8$ bar, ethane: $T_c = 32.2\,°C$, $p_c = 48.8$ bar) and 73–87% in hexane. An uncomfortable feature of the reaction was the gradual loss of activity though deactivation was less pronounced at low total pressures [41]. In the following, the influence of solvents on catalyst deactivation is compared at 190 bar and 40 °C (i.e., slightly above the critical temperature of CO_2 and ethane). Former phase behavior measurements of the system in a high-pressure view cell showed that under these conditions the reaction mixture was made up of a single phase (supercritical region) [41].

The time-dependent variations of conversion and selectivities to citronellal, 3,7-dimethyl-2-octenal, and dihydrocitronellal in dense carbon dioxide are shown in Fig. 1. The conversion decreased by about 17% in the 4-h period presented. The considerable shift in the product distribution indicates that the loss of catalytic activity cannot simply be attributed to a decrease of the number of active surface sites. After 1 h the dominant product was the saturated aldehyde dihydrocitronellal (**4**) and after 5 h the α,β-unsaturated aldehyde 3,7-dimethyl-2-octenal (**3**) formed with the highest selectivity. The decreasing fraction of dihydrocitronellal can be attributed partly to the lower conversion and the total hydrogen uptake (not shown). Note that dihydrocitronellal (**4**) is not an intermediate but a final product under applied conditions. A possible change in the reaction orders of the various steps in Scheme 1 due to the catalyst deactivation cannot be ruled out. The shift in the product distribution is best illustrated by the time dependence of the molar ratio 3,7-dimethyl-2-octenal/citronellal (**3**/**2**). An increase of this ratio from 0.35 to 0.56 during the 4-h period indicates the rate of saturation of the isolated C=C bond of citral increased relative to that of the allylic C=C bond. Note that no stabilization of the catalyst could be achieved even after 40 h time on stream.

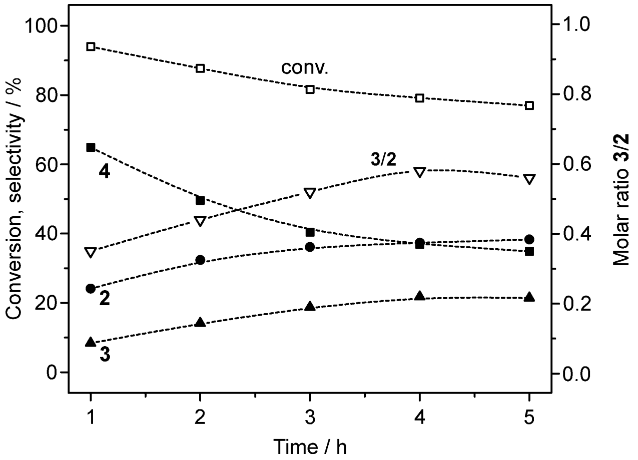

Fig. 1. Catalyst deactivation during hydrogenation of citral (**1**) in “supercritical” CO_2, illustrated by the changes of conversion and selectivities to citronellal (**2**), 3,7-dimethyl-2-octenal (**3**), and dihydrocitronellal (**4**); standard conditions.

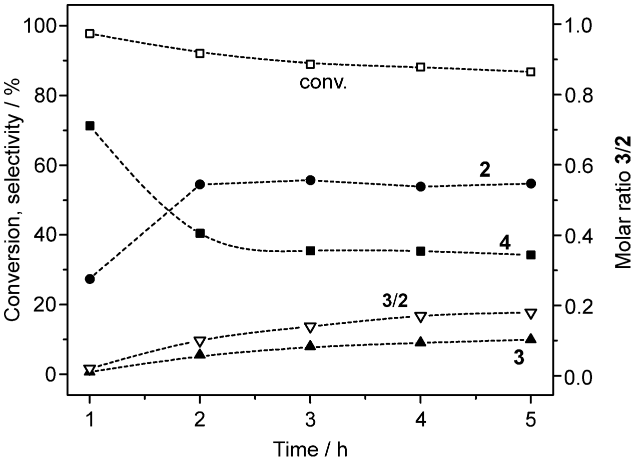

Fig. 2. Catalyst deactivation during hydrogenation of citral (**1**) in “supercritical” ethane and the resulting shifts in selectivities to citronellal (**2**), 3,7-dimethyl-2-octenal (**3**), and dihydrocitronellal (**4**); standard conditions.

Changes in the selectivity pattern of Pd/Al_2O_3 with time on stream were typical for all three solvents. The increase of the molar ratio 3,7-dimethyl-2-octenal/citronellal (**3**/**2**, from 0.02 to 0.18) was most pronounced in supercritical ethane

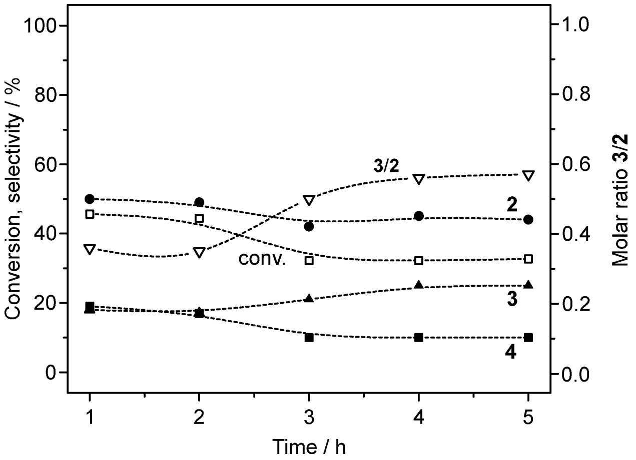

Fig. 3. Catalyst deactivation during hydrogenation of citral (**1**) in hexane, illustrated by the changes of conversion and selectivities to citronellal (**2**), 3,7-dimethyl-2-octenal (**3**), and dihydrocitronellal (**4**); standard conditions.

(Fig. 2). In contrast, catalyst deactivation was modest in this solvent; in 4 h the citral conversion decreased by only 11%. In the apolar conventional solvent hexane (Fig. 3) the conversion decreased by about 13% and after 3–4 h a steady state in conversion and selectivities was reached. When considering the moderate conversion in hexane, then the relative loss of catalyst activity seems to be the highest in this solvent. The very low selectivity to the saturated aldehyde dihydrocitronellal is also mainly due to the low conversion of citral.

In all three solvents, deactivation of Pd/Al_2O_3 was minor compared to those cases reported earlier. Singh and Vannice [32] investigated the liquid-phase hydrogenation of citral over Pt/SiO_2 in a batch reactor at 25 °C and observed a drop of more than an order of magnitude in the reaction rate in the first 4 h. Later, Murzin and co-workers [33] studied the reaction in ethanol at 70 °C, also in a batch reactor. The activity of a Ru/Al_2O_3 catalyst decreased by two orders of magnitude in 5 h.

3.2. *Reactivation of Pd/Al_2O_3 by oxidation in air*

Lercher and co-workers [49] suggested that deactivation of Pt/SiO_2 in the hydrogenation of crotonaldehyde to crotylalcohol was due to decarbonylation of the α, β-unsaturated aldehyde and irreversible adsorption of CO on the Pt sites. Indirect evidence to this assumption was given by oxidation of adsorbed CO to CO_2 with air, treatment of which resulted in the regeneration of the initial activity of the catalyst. Applying the same approach, Singh and Vannice [10] could regenerate Pt/SiO_2 in the hydrogenation of citral. In both cases, the activity dropped again when the hydrogenation continued, in good agreement with the proposed decarbonylation of the aldehyde reactant and the accumulation of CO on the reduced metal surface.

We also attempted to reactivate the catalyst by an oxidative treatment. The experiment shown in Fig. 1 was repeated and after 3 h time on stream the mass flows were stopped and the catalyst bed was flushed with air for 10 min. As illustrated in Fig. 4, oxidation with air could not regenerate the initial activity of Pd/Al_2O_3 though improved the conversion by ca. 2%. What is more important, after about 1 h stabilization further catalyst deactivation ceased and the citral conversion and the selectivities to **2**–**4** reached steady-state values. Apparently, Pd/Al_2O_3 behaves remarkably different compared to Pt/SiO_2.

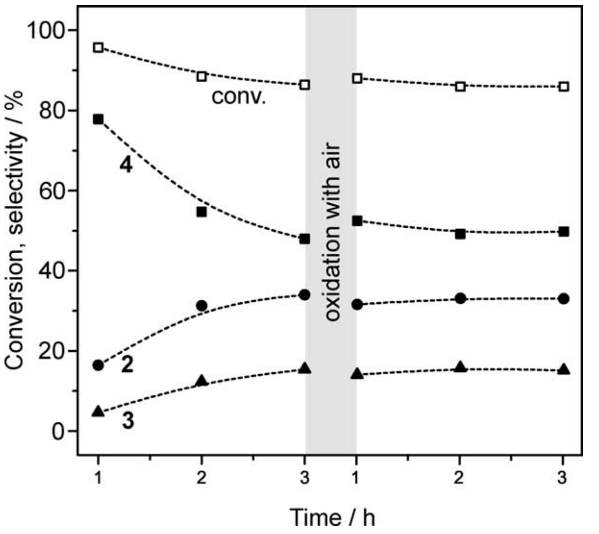

Fig. 4. The influence of catalyst reactivation with air during citral (**1**) hydrogenation in "supercritical" CO_2. The changes of conversion and selectivities to citronellal (**2**), 3,7-dimethyl-2-octenal (**3**), and dihydrocitronellal (**4**) were determined under standard conditions. Reactivation consisted of flushing the catalyst bed with air for 10 min.

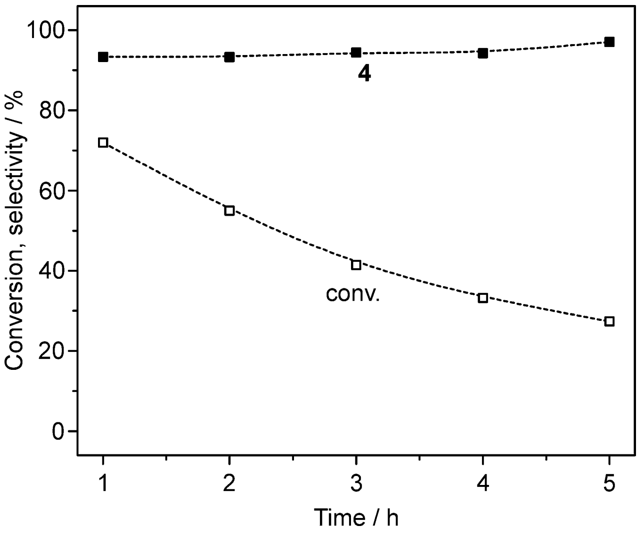

Fig. 5. Catalyst deactivation during hydrogenation of citronellal (**2**) and the selectivity to dihydrocitronellal (**4**) in "supercritical" CO_2; standard conditions.

3.3. *Deactivation of Pd/Al_2O_3 during hydrogenation of citronellal*

Finally, catalyst deactivation in the hydrogenation of citronellal (**2**) was investigated in supercritical carbon dioxide

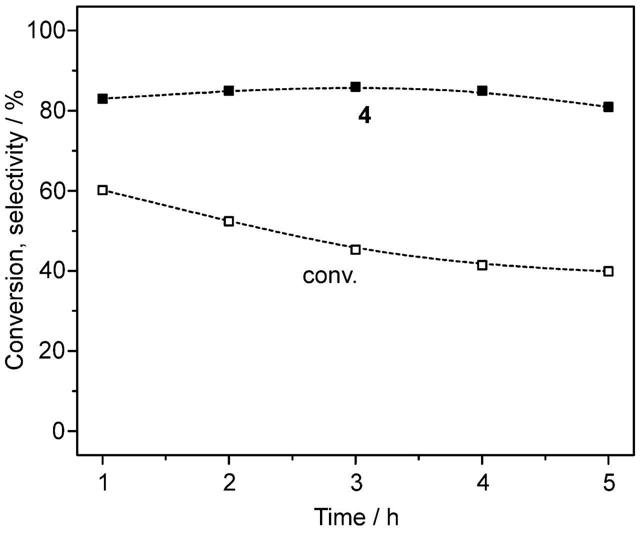

Fig. 6. Catalyst deactivation during hydrogenation of citronellal (**2**) in hexane and the selectivity to dihydrocitronellal (**4**); standard conditions but with 0.25 g catalyst due to the low reaction rate in this solvent.

(Fig. 5) and in hexane (Fig. 6). A comparison of Figs. 1 and 5, as well as Figs. 3 and 6, shows that in both solvents catalyst deactivation was more severe in citronellal hydrogenation than in citral hydrogenation. For example, in carbon dioxide the conversion decreased by more than 45% in 4 h during citronellal hydrogenation (Fig. 5) but only by 17% during citral hydrogenation (Fig. 1).

3.4. *ATR-IR spectroscopy*

We used ATR-IR spectroscopy to detect CO at the solid/liquid interface and thus to clarify the importance of decarbonylation reactions during citral hydrogenation. The measurements were carried out using an in-house-built stainless-steel flow cell under conditions similar to those applied in the continuous-flow fixed-bed reactor, except that the total pressure was 1 bar. Hydrogen was introduced by saturation of the hexane solution at 1 bar. The hydrogen-saturated hexane solution of citral, citronellal, dihydrocitronellal, geraniol, or nerol was pumped through the reactor cell containing a thin catalyst film deposited on a ZnSe internal reflection element. The spectra were recorded while flowing one of these solutions through the cell. For each reactant, a fresh catalyst film was prepared and used. Spectra of citral, citronellal, dihydrocitronellal, geraniol, and nerol in hexane solutions were also taken in the transmission mode.

Fig. 7 shows the spectra of the interaction of citral with the reduced catalyst. The spectra evidence that the 5 wt% Pd/Al_2O_3 really catalyzed the hydrogenation of citral under the conditions applied in the ATR-IR reactor cell. The small band observed at 1734 cm^{-1} can be assigned to the $\nu(C{=}O)$ band of the dissolved hydrogenated products citronellal and dihydrocitronellal in which compounds the C=O bond is not associated with a C=C bond in α-position. The two products cannot be clearly distinguished since they both display the C=O stretching vibration at 1734 cm^{-1}. The signal at 1686 cm^{-1} in Fig. 7 corresponds to the $\nu(C{=}O)$ mode of dissolved citral.

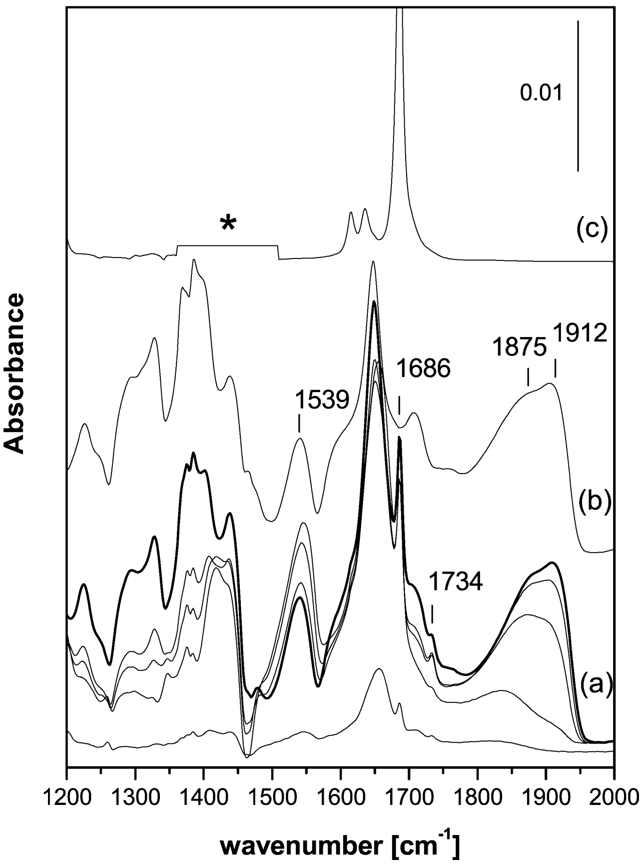

Fig. 7. (a) ATR-IR spectra of CO evolution during hydrogenation of citral in hexane on Pd/Al_2O_3. The time elapsed between the first and last spectrum (bold) is 17 min. (b) ATR-IR spectrum of adsorbed species after washing with neat solvent for 10 min. (c) Minimized transmission FTIR spectrum of dissolved citral in hexane (1:100). The spectral range marked by an asterisk is covered by strong solvent bands.

The relatively broad band at ca. 1650 cm^{-1}, growing in with time, is assigned to citral adsorbed onto Al_2O_3. In addition, adsorbed carboxylate species were also formed as indicated by the signal at 1539 cm^{-1} ($\nu(COO)_{as}$) and possibly by that at 1420 cm^{-1}. These bands were found to slightly attenuate during the experiment. In the 1300–1450 cm^{-1} region several overlapping bands evolved, whose precise assignment to specific adsorbed species is rather difficult. However, note that the overall intensity of this envelope increases with time in contrast to the bands at 1539 and 1420 cm^{-1}. Formation of carboxylic acid may be attributed to disproportionation (Cannizzaro reaction) of the aldehyde reactant on the basic sites of alumina. We could never detect even traces of geranic acid by GC analysis of the products that may indicate strong adsorption of this by-product on the basic sites of the catalyst.

Furthermore, two bands at around 1912 and 1875 cm^{-1} evolved during interaction of citral with the reduced Pd surface. They are associated with (bridged) CO species ad-

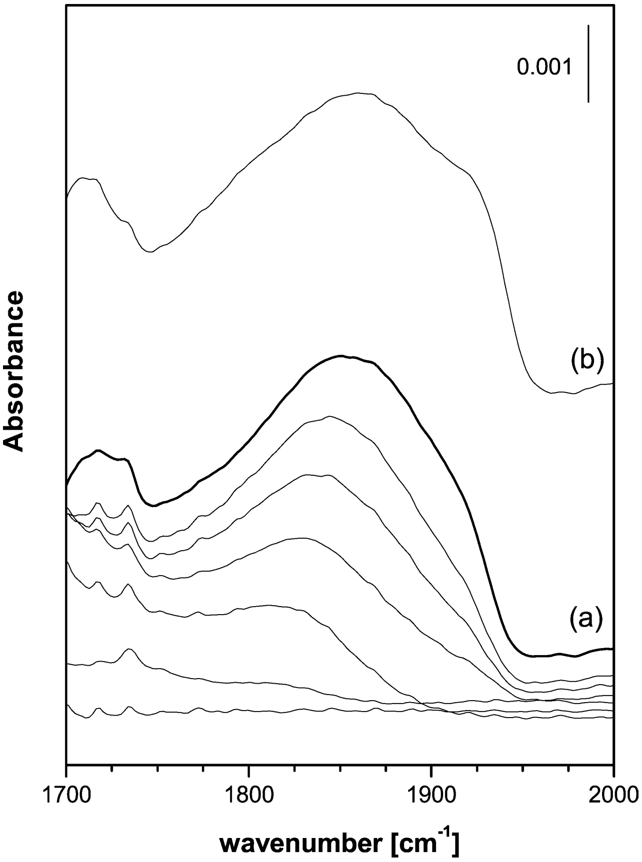

Fig. 8. (a) ATR-IR spectra of CO evolution during hydrogenation of nerol in hexane on Pd/Al_2O_3. The time elapsed between the first and last spectrum (bold) is 33 min. (b) ATR-IR spectrum of adsorbed species after washing with neat solvent for 15 min.

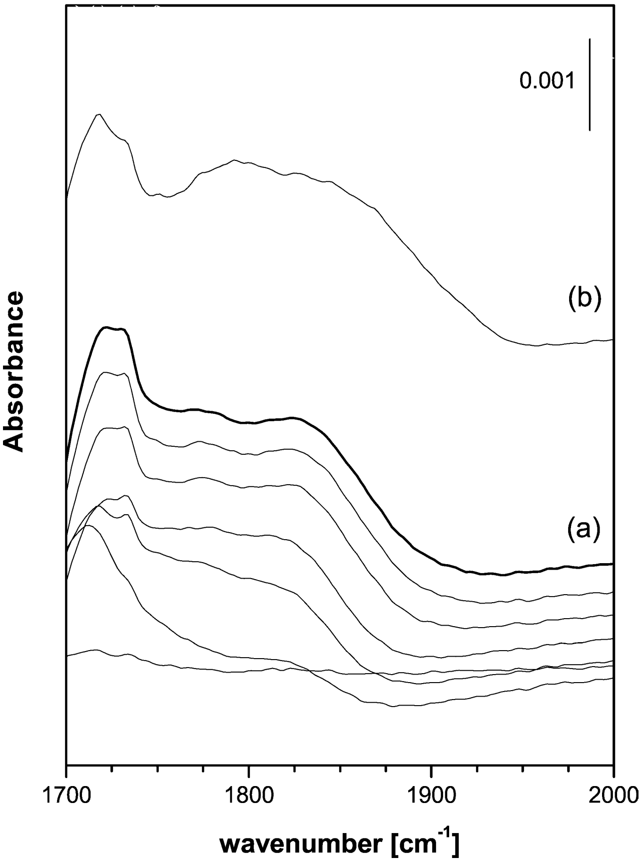

Fig. 9. (a) ATR-IR spectra of CO evolution during hydrogenation of geraniol in hexane on Pd/Al_2O_3. The time elapsed between the first and last spectrum (bold) is 26 min. (b) ATR-IR spectrum of adsorbed species after washing with neat solvent for 10 min.

sorbed on (polycrystalline) Pd [39]—a clear evidence for decarbonylation of citral on the Pd surface. The characteristic CO bands were detected though to a smaller extent when nerol (Fig. 8) or geraniol (Fig. 9) was fed in the reactor cell. Decarbonylation of nerol seems to be faster than that of the thermodynamically more stable isomer geraniol. Interestingly, no CO formation was observed when the catalyst was exposed to a flow of hexane containing citronellal (Fig. 10) or dihydrocitronellal (Fig. 11).

Rinsing of the catalyst layer by hexane solvent caused the disappearance of the bands due to dissolved species, namely at 1734 and 1686 cm^{-1}. Fig. 7b shows that CO, citral, and carboxylate-containing species remained on the catalyst surface. Additionally, the composite envelope below 1450 cm^{-1} is also observed.

4. Discussion

Studies of the decomposition of saturated and α,β-unsaturated alcohols and aldehydes on clean Pd single-crystal surfaces in vacuum [34,35,40,50] showed that the major reaction pathway is decarbonylation via an acyl species (Scheme 2), and the reactivities of aliphatic and vinylic oxygenates are similar [51]. In contrast, ATR-IR studies in the presence of solvent (hexane) and hydrogen (at 1 bar) revealed characteristic differences in the reactivity of citral and its partially hydrogenated derivatives (Scheme 1) over the surface of Pd/Al_2O_3. Most importantly, citronellal and dihydrocitronellal did not decarbonylate on Pd under the conditions applied (Figs. 7–11). A closer supervision of the structure and reactivity of all compounds investigated by ATR-IR indicates that only the α,β-unsaturated alcohols (geraniol, nerol) and aldehydes (citral, 3,7-dimethyl-2-octenal) decarbonylated on Pd/Al_2O_3.

Another important information derived from the catalytic experiments is the excellent selectivity of Pd in the saturation of the C=C bonds of citral in all three weakly polar solvents applied (Figs. 7–11). Hydrogenation of the C=O bonds was not detectable by GC, in agreement with some recent reports of citral hydrogenation on Pd/Al_2O_3 in supercritical carbon dioxide [25,41].

The catalytic and ATR-IR spectroscopic studies may be explained by assuming specific adsorption modes of citral and its hydrogenated derivatives on the supported Pd particles (Scheme 3). We assume that only those molecules adsorb sufficiently strongly and are hydrogenated on Pd that

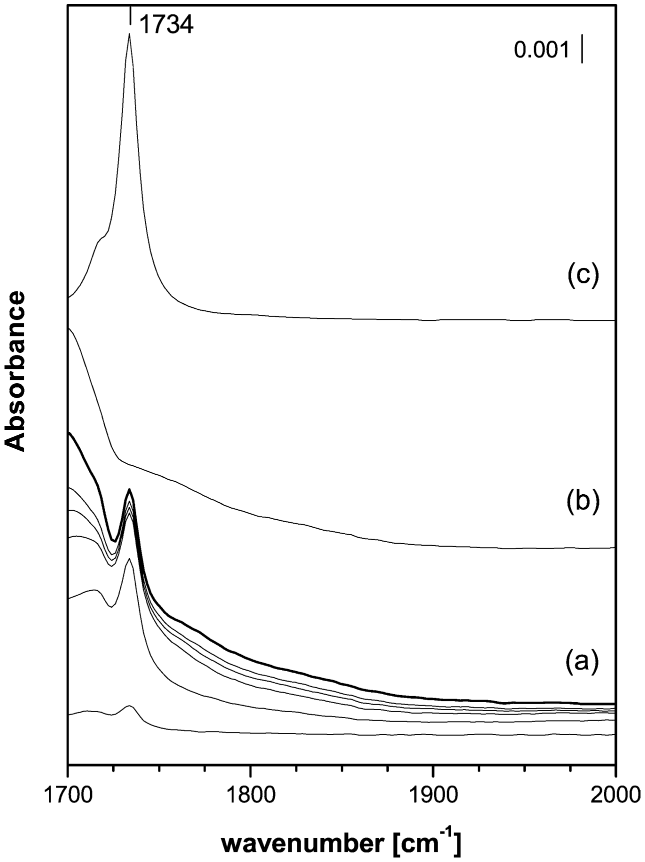

Fig. 10. (a) ATR-IR spectra taken during hydrogenation of citronellal in hexane on Pd/Al_2O_3. The time elapsed between the first and last spectrum (bold) is 24 min. (b) ATR-IR spectrum of adsorbed species after washing with neat solvent for 8 min. (c) Minimized transmission FTIR spectrum of dissolved citronellal in hexane (1:100).

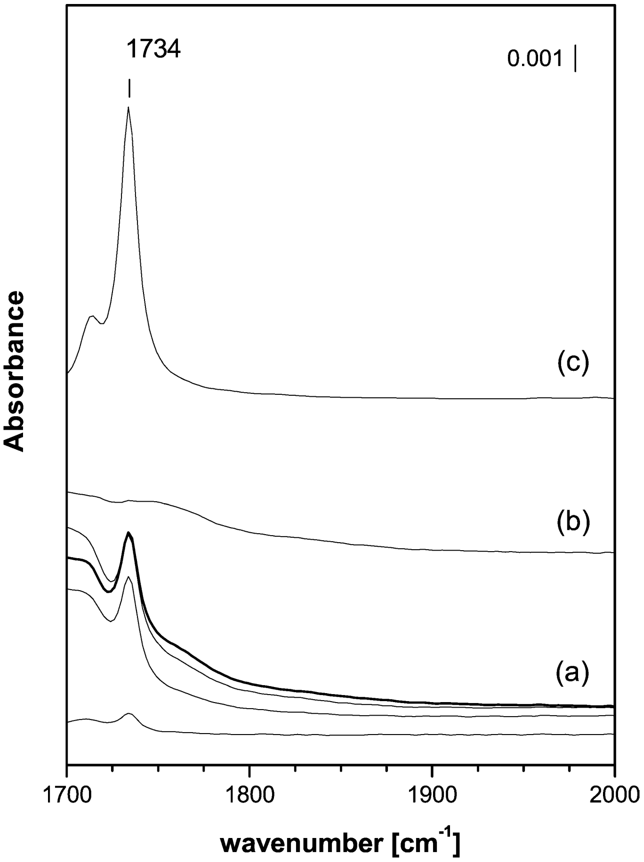

Fig. 11. (a) ATR-IR spectra taken during adsorption of dihydrocitronellal in hexane on Pd/Al_2O_3. The time elapsed between the first and last spectrum (bold) is 26 min. (b) ATR-IR spectrum of adsorbed species after washing with neat solvent for 11 min. (c) Minimized transmission FTIR spectrum of dissolved dihydrocitronellal in hexane (1:100).

possess a C=C bond. The unsaturated aldehydes and alcohols citral (**1**), geraniol (**5**), and nerol (**6**) would adsorb on Pd in a tilted position via only one of the C=C bonds due to the strong competition for the active sites under the reaction conditions. In this way the overall adsorption-free enthalpy change is maximized. Adsorption of citral (**1**) via the isolated C=C bond leads to 3,7-dimethyl-2-octenal (**3**) upon hydrogen uptake (Scheme 3a). Adsorption of citral (**1**) or 3,7-dimethyl-2-octenal (**3**) via the allylic C=C bond is assumed to involve also the C=O bond (di-$\pi\eta_2$ bonding [52]). This adsorption mode allows either the hydrogenation of the C=C bond and desorption of the aldehyde or the decarbonylation to CO and hydrocarbon fragments (Scheme 3a and b). As shown in Scheme 3c, citronellal (**2**) would adsorb via the C=C bond and be hydrogenated to dihydrocitronellal (**4**) but the latter saturated aldehyde is unreactive under the reaction conditions, as indicated by the catalytic data. In the suggested adsorption mode of citronellal (**2**) no decarbonylation can occur.

We can partly confirm the recent proposal by Singh and Vannice [10,32] that catalyst deactivation during citral hydrogenation would be due to decarbonylation of citral, geraniol, or nerol. These three compounds decarbonylate also on Pd/Al_2O_3 as indicated by the ATR-IR spectroscopic analysis. The catalytic experiments in Figs. 1–6 show, however, that deactivation of Pd/Al_2O_3 is more complex and only decarbonylation and CO poisoning cannot interpret the experimental observations. Deactivation of Pd/Al_2O_3 was far more extensive in the hydrogenation of citronellal than in the hydrogenation of citral though citronellal does not decarbonylate on Pd (Fig. 10). Besides, an oxidative treatment could not regenerate the original activity of Pd/Al_2O_3, indicating that CO poisoning is not the major reason of catalyst deactivation and is not connected with the irreversible loss of activity with time on stream.

We do not have an unambiguous explanation yet for the deactivation of Pd/Al_2O_3. We assume that dimerization and oligomerization of citral, its partially hydrogenated products, or those of the hydrocarbon fragments originating from the decarbonylation reactions, may produce strongly adsorbed species that gradually cover a fraction of the active sites. The ATR-IR spectra of the interactions of citral, nerol, and geraniol with Pd/Al_2O_3 showed some bands in the region 1300–1450 cm^{-1} whose intensity increased with time on stream. This is the region where δ(C–H) vibrations are expected. The $\nu(COO)_{sym}$ of carboxylate species and citral

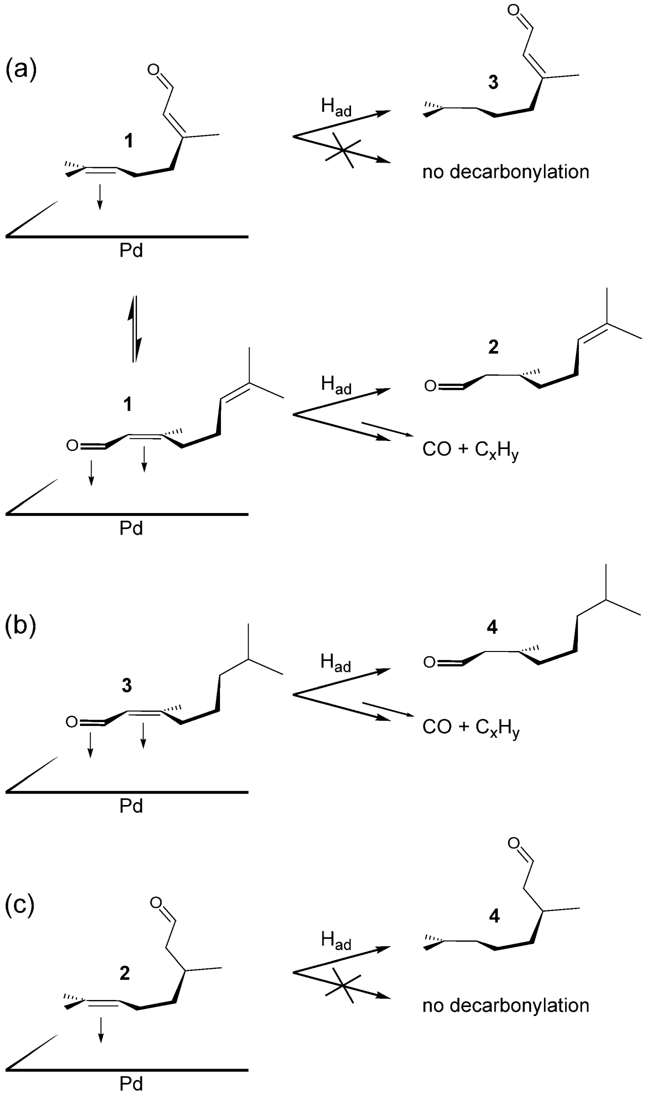

Scheme 3. Schematic representation of the proposed adsorption modes and reactivities of citral (**1**), citronellal (**2**), 3,7-dimethyl-2-octenal (**3**), and dihydrocitronellal (**4**) on alumina-supported Pd particles.

itself also show features in this region. However, since the $\nu(COO)_{as}$ band decreases with time during citral adsorption and some other bands cannot be assigned to adsorbed citral due to their relative strong intensity, it seems that some other species are also present on the surface even after rinsing the catalyst with the solvent. We tentatively assign these bands to oligomeric species accumulating on the catalyst surface. We further speculate that the small amount of carboxylic acid by-product may catalyze dimerization. Obviously, an oxidative treatment under very mild conditions cannot remove these strongly adsorbed species, as shown in Fig. 4.

5. Conclusions

Hydrogenation of citral (**1**) in supercritical solvents on a 5 wt% Pd/Al_2O_3 catalyst in a continuous-flow fixed-bed reactor is characterized by high selectivity to the hydrogenation of the C=C bonds of the unsaturated aldehyde and a gradual loss of activity with time on stream. Catalyst deactivation could not be avoided by varying the reaction conditions including the solvents (supercritical carbon dioxide and ethane, and hexane). A short aerobic oxidation of the used catalyst under mild conditions, however, terminated further loss of activity.

Two major reasons of catalyst deactivation are suggested on the basis of the catalytic experiments and ATR-IR spectroscopic investigation of the Pd/Al_2O_3/hexane interface. Decarbonylation of the α, β-unsaturated aldehydes citral and 3,7-dimethyl-2-octenal provides strongly adsorbed CO and hydrocarbon fragments. In contrast, the other two major products citronellal and dihydrocitronellal do not decompose on Pd. The failed catalyst reactivation with air and the strongest deactivation of Pd/Al_2O_3 observed in the hydrogenation of citronellal (**2**) indicate that decarbonylation alone cannot account for the observed loss of activity. We assume that dimerization and oligomerization of citral and its partially hydrogenated derivatives, as well as the hydrocarbon fragments formed in the decarbonylation reactions, result in extensive site blocking and irreversible deactivation.

Acknowledgments

Financial support by the Bundesamt für Energie (BFE) is gratefully acknowledged. Thanks are also due to Dr. D. Ferri for valuable help with the ATR-IR investigations.

References

[1] P. Claus, Top. Catal. 5 (1998) 51.
[2] P. Gallezot, D. Richard, Catal. Rev.-Sci. Eng. 40 (1998) 81.
[3] V. Ponec, Appl. Catal. A 149 (1997) 27.
[4] G. Neri, L. Mercadante, A. Donato, A.M. Visco, S. Galvagno, Catal. Lett. 29 (1994) 379.
[5] S. Galvagno, C. Milone, G. Neri, A. Donato, R. Pietropaolo, Stud. Surf. Sci. Catal. 78 (1993) 163.
[6] N. Ravasio, M. Antenori, F. Babudri, M. Gargano, Stud. Surf. Sci. Catal. 108 (1997) 625.
[7] U.K. Singh, M.N. Sysak, M.A. Vannice, J. Catal. 191 (2000) 181.
[8] P. Maki-Arvela, L.P. Tiainen, A.K. Neyestanaki, R. Sjoholm, T.K. Rantakyla, E. Laine, T. Salmi, D.Y. Murzin, Appl. Catal. A 237 (2002) 181.
[9] A.M. Pak, D.V. Sokolskii, S.R. Konuspaev, Kinet. Catal. 21 (1980) 491.
[10] U.K. Singh, M.A. Vannice, J. Catal. 199 (2001) 73.
[11] C. Milone, M.L. Tropeano, G. Gulino, G. Neri, R. Ingoglia, S. Galvagno, Chem. Commun. (2002) 868.
[12] U.K. Singh, M.A. Vannice, J. Mol. Catal. A: Chem. 163 (2000) 233.
[13] R. Malathi, R.P. Viswanath, Appl. Catal. A 208 (2001) 323.
[14] J. Court, F. Janatiidrissi, S. Vidal, P. Wierzchowski, J. Chim. Phys.-Chim. Biol. 87 (1990) 379.
[15] B. Didillon, J.P. Candy, A. Elmansour, C. Houtmann, J.M. Basset, J. Mol. Catal. 74 (1992) 43.
[16] S. Galvagno, C. Milone, A. Donato, G. Neri, R. Pietropaolo, Catal. Lett. 17 (1993) 55.

[17] G. Neri, L. Mercadante, C. Milone, R. Pietropaolo, S. Galvagno, J. Mol. Catal. A: Chem. 108 (1996) 41.

[18] J.N. Coupe, E. Jordao, M.A. Fraga, M.J. Mendes, Appl. Catal. A 199 (2000) 45.

[19] P. Reyes, H. Rojas, G. Pecchi, J.L.G. Fierro, J. Mol. Catal. A: Chem. 179 (2002) 293.

[20] P. Maki-Arvela, L.P. Tiainen, M. Lindblad, K. Demirkan, N. Kumar, R. Sjoholm, T. Ollonqvist, J. Vayrynen, T. Salmi, D.Y. Murzin, Appl. Catal. A 241 (2003) 271.

[21] B. Bachiller-Baeza, A. Guerrero-Ruiz, P. Wang, I. Rodriguez-Ramos, J. Catal. 204 (2001) 450.

[22] L. Sordelli, R. Psaro, G. Vlaic, A. Cepparo, S. Recchia, C. Dossi, A. Fusi, R. Zanoni, J. Catal. 182 (1999) 186.

[23] M.A. Aramendia, V. Borau, C. Jimenez, J.M. Marinas, A. Porras, F.J. Urbano, J. Catal. 172 (1997) 46.

[24] K. Anderson, P. Goodrich, C. Hardacre, D.W. Rooney, Green Chem. 5 (2003) 448.

[25] M. Chatterjee, A. Chatterjee, Y. Ikushima, Green Chem. 6 (2004) 114.

[26] M. Chatterjee, F.Y. Zhao, Y. Ikushima, Adv. Synth. Catal. 346 (2004) 459.

[27] P. Maki-Arvela, L.P. Tiainen, R. Gil, T. Salmi, Stud. Surf. Sci. Catal. 108 (1997) 273.

[28] L.P. Tiainen, P. Maki-Arvela, T. Salmi, Catal. Today 48 (1999) 57.

[29] A.M. Silva, O.A.A. Santos, M.J. Mendes, E. Jordao, M.A. Fraga, Appl. Catal. A 241 (2003) 155.

[30] S. Recchia, C. Dossi, A. Fusi, L. Sordelli, R. Psaro, Appl. Catal. A 182 (1999) 41.

[31] J. Aumo, J. Lilja, P. Maki-Arvela, T. Salmi, M. Sundell, H. Vainio, D.Y. Murzin, Catal. Lett. 84 (2002) 219.

[32] U.K. Singh, M.A. Vannice, J. Catal. 191 (2000) 165.

[33] L.P. Tiainen, P. Maki-Arvela, A.K. Neyestanaki, T. Salmi, D.Y. Murzin, React. Kinet. Catal. Lett. 78 (2003) 251.

[34] J.L. Davis, M.A. Barteau, J. Am. Chem. Soc. 111 (1989) 1782.

[35] R. Shekhar, M.A. Barteau, R.V. Plank, J.M. Vohs, J. Phys. Chem. B 101 (1997) 7939.

[36] J.F.E. Gootzen, A.H. Wonders, A.P. Cox, W. Visscher, J.A.R. van Veen, J. Mol. Catal. A: Chem. 127 (1997) 113.

[37] J.C. de Jesus, F. Zaera, Surf. Sci. 430 (1999) 99.

[38] M. Bron, R. Holze, Surf. Sci. 457 (2000) 178.

[39] C. Keresszegi, T. Bürgi, T. Mallat, A. Baiker, J. Catal. 211 (2002) 244.

[40] J.L. Davis, M.A. Barteau, Surf. Sci. 235 (1990) 235.

[41] M. Burgener, R. Furrer, T. Mallat, A. Baiker, Appl. Catal. A 268 (2004) 1.

[42] N.J. Harrick, Internal Reflection Spectroscopy, Interscience, New York, 1967.

[43] D. Ferri, T. Bürgi, A. Baiker, J. Phys. Chem. B 105 (2001) 3187.

[44] T. Bürgi, A. Baiker, J. Phys. Chem. B 106 (2002) 10649.

[45] R. Tschan, R. Wandeler, M.S. Schneider, M.M. Schubert, A. Baiker, J. Catal. 204 (2001) 219.

[46] R. Wandeler, N. Künzle, M.S. Schneider, T. Mallat, A. Baiker, J. Catal. 200 (2001) 377.

[47] J.S. Rowlinson, F.L. Swinton, Liquids and Liquid Mixtures, third ed., Butterworth, London, 1982.

[48] A. Urakawa, R. Wirz, T. Bürgi, A. Baiker, J. Phys. Chem. B 107 (2003) 13061.

[49] M. Englisch, V.S. Ranade, J.A. Lercher, Appl. Catal. A 163 (1997) 111.

[50] R. Shekhar, M.A. Barteau, Surf. Sci. 319 (1994) 298.

[51] J.L. Davis, M.A. Barteau, J. Mol. Catal. 77 (1992) 109.

[52] F. Delbecq, P. Sautet, J. Catal. 152 (1995) 217.